ELSEVIER

Density functional and ab initio study of the tautomeric forms of 3-acetyl tetronic and 3-acetyl tetramic acids

Chris-Kriton Skylaris [a,*], Olga Igglessi-Markopoulou [b], Anastasia Detsi [b], John Markopoulos [c]

[a] *Theory of Condensed Matter group, Cavendish Laboratory, Madingley Road, Cambridge CB3 0HE, UK*
[b] *Laboratory of Organic Chemistry, Department of Chemical Engineering, National Technical University of Athens, Zografou Campus, GR-15773 Athens, Greece*
[c] *Laboratory of Inorganic Chemistry, Department of Chemistry, University of Athens, Panepistimiopolis, GR-15771 Athens, Greece*

Abstract

We propose all the accessible paths of interconversion between the tautomers of 3-acetyl tetronic and 3-acetyl tetramic acids by performing calculations with the density functional B3LYP method and the ab initio MP2 method. Our findings clarify at the atomic level the mechanisms of the equilibria between these tautomers, a topic so far only partially understood on the basis of studies by nuclear magnetic resonance (NMR) spectroscopy. We show that thermal effects via relative Gibbs free energies ΔG must be taken into account in order to reach good quantitative agreement with the available experimental information on the ratios of the most stable tautomers. The calculated ^{1}H and ^{13}C chemical shifts are in agreement with the experimental values from NMR spectroscopy.
© 2003 Elsevier B.V. All rights reserved.

1. Introduction

The 3-acyl tetronic and 3-acyl tetramic acids are a class of five-membered ring heterocycles frequently encountered in natural products, which exhibit diverse biological activity [1,2]. Representative examples of 3-acyl tetronic acids include the antitumor antibiotics tetrocarcins [3], quartromicins with antibiotic and antiviral activity against herpes virus type 1 and HIV [4] and the potent tyrosine phosphatase inhibitor RK-682 [5]. Members of the 3-acyl tetramic acid group of compounds such as tenuazonic acid, tirandamycin, streptolydigin, ikaguramycin [2], melophlins A and B [6], cryptocin [7] and the recently isolated militarinones B and C [8] reportedly have antiviral, antitumor, antibiotic and antimicrobial activity as well as cytotoxicity and mycotoxicity.

The structures of 3-acetyl tetronic acid and of 3-acetyl tetramic acid are shown in Fig. 1. All other 3-acyl tetronic and 3-acyl tetramic acids can be considered as resulting from substitution of the hydrogens of C5 with other functional groups and
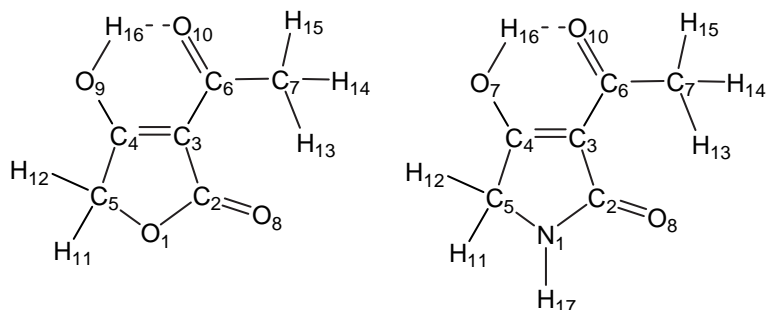

Fig. 1. Left: The structure of 3-acetyl tetronic acid including its atom numbering scheme. Right: 3-acetyl tetramic acid.

also by substitution of the methyl group of C7. Furthermore, 3-acyl tetramic acids present the possibility to attach functional groups to their nitrogen atom by replacing H17.

The 3-acyl tetronic and 3-acyl tetramic acids are strongly acidic (pK_a values of 3.0 or less) as they contain a methine carbon connected to three carbonyl groups [2]. They are formally β,β'-tricarbonyl systems and they are able to form many keto–enol tautomers. The knowledge of the relative stability and interconversion mechanisms of their tautomers can assist in the interpretation of their chemical behaviour in order to discover methods for their synthesis [9–15]. Furthermore, there are applications in organometallic chemistry and catalysis as the β,β'-tricarbonyl structure of these acids means that they are very efficient as bidentate ligands and can substitute commonly used β-dicarbonyl ligands from a variety of transition metal complexes [16–18]. Observations of these acids in nonpolar solvents (e.g., CDCl$_3$), mainly by nuclear magnetic resonance (NMR) spectroscopy, show the presence of more than one tautomer [19,20].

The only theoretical study of these compounds so far to our knowledge has been the work of Broughton and Woodward [21] who performed calculations with the AM1 [22] semiempirical method on 3-acetyl tetronic and 3-acetyl tetramic acid. They found that the tautomers of 3-acetyl tetronic acid shown in Fig. 2 were more stable by at least 40 kJ/mol from the doubly enolised tautomers (not shown in Fig. 2). It should be noted that structures **r1**, **r2** and **r3** are just rotamers of the unenolised species. A set of structures equivalent to those of Fig. 2 were also located for 3-acetyl
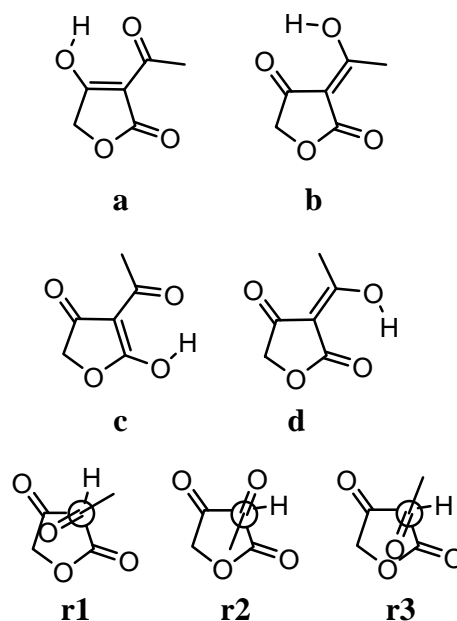

Fig. 2. The most stable tautomers of 3-acetyl tetronic acid.

tetramic acid except for structure **r3** which did not converge to a minimum [21].

The energies of tautomers **b** and **d** were less than 4 kJ/mol apart and lower by more than 20 kJ/mol from the energies of all other tautomers, for the 3-acetyl tetronic as well as for the 3-acetyl tetramic acid. On this basis, Broughton and Woodward concluded that **b** and **d** would be the predominant tautomers in CDCl$_3$ solutions as two species have been observed by NMR spectroscopy in solution for 3-acetyl tetronic [19,36] and 3-acetyl tetramic [9,20] acids.

It has been proposed [20] that the interconversion between the "internal" tautomers **a** and **b** is too rapid to be observed on the NMR timescale. Likewise for the "internal" tautomers **c** and **d**. The interconversion between the "external" tautomers (**a**, **b**) and (**c**, **d**) is slower as has been deduced on the basis of NMR spectra [20], so the two signals observed should actually be the weighted averages of the (**a**, **b**) and (**c**, **d**) pairs.

In this work we advance the theoretical study of 3-acetyl tetronic and 3-acetyl tetramic acids by performing calculations with highly accurate correlated ab initio and density functional methods. We calculate the relative stabilities of the tautomers of Fig. 2 and determine the paths and energetics for their interconversion including the transition states that are involved in each step. We also calculate NMR spectra for the abundant tautomers and compare them to experimental assignments.

2. Computational details

The geometries of all structures were optimised with the density functional theory method with the B3LYP [23] hybrid functional whose high accuracy has been demonstrated for a large variety of organic compounds [24]. No symmetry constraints were applied (point group C_1). The energy of each optimised structure obtained was re-computed by rotating the methyl group of C7 (see Fig. 1) until the lowest rotameric minimum was located and then the whole structure was re-optimised. The pVDZ basis set was used for these tasks as the best compromise between accurate structures and affordable computational cost [25]. It was verified that all the vibrational frequencies of each equilibrium structure were real. Similarly, it was verified that only one of the vibrational frequencies of each transition state was imaginary. In order to represent the potential energy surface as accurately as possible, very tight convergence thresholds were applied in the calculation of energies and geometries (energies converged to 1.0×10^{-10} E_h and gradients to 1.5×10^{-5} E_h/a_0). Ab initio second order Møller–Plesset perturbation theory (MP2) and B3LYP energetics were obtained from single

point calculations at the optimised structures with the larger pTZV basis set [26] which was designed to improve the energies obtained with the pVDZ basis. All geometry optimisations and single point energy calculations were carried out with the NWChem 4.1 computational chemistry package [27]. Nuclear magnetic resonance (NMR) chemical shifts were calculated with the GIAO [28] SCF method using the Dalton 1.2 Quantum Chemistry program [29]. The pTZV basis was also used in the GIAO SCF calculations as it has been shown to produce chemical shifts with maximum errors less than 5% from the Hartree–Fock complete basis set limit [30].

3. Results and discussion

We began our exploration of the potential energy surface of 3-acetyl tetronic acid by an initial approximation for tautomer **a** of Fig. 2 which converged into the structure **a** shown in Fig. 3. A transition state search along the normal modes of structure **a** that lead to chemically plausible structures produced the transition state structures **a–b TS** and **a–r1 TS** of Fig. 3. By proceeding in this fashion all the structures shown in the scheme of Fig. 3 were obtained. We should note that the scheme of Fig. 3 can also be obtained if either of the structures **b**, **c** or **d** is used as an initial approximation instead of structure **a**. All the optimised structures of 3-acetyl tetronic acid are presented in the scheme of Fig. 3 that demonstrates the available paths for interconversion between tautomers **a**, **b**, **c**, **d** and rotamers **r1**, **r2**, **r3**. This is the mechanism of the tautomerisation reactions of 3-acetyl tetronic acid in vacuum or in aprotic solvents where there is no participation of the solvent in the rearrangements of the acidic proton of the molecule.

Eight transition states were found: **a–b TS**, **c–d TS**, **b–d TS**, **a–r1 TS**, **(b, d)–r2 TS**, **c–r3 TS**, **r1–r2 TS** and **r2–r3 TS**. Structure **a–b TS** connects "internal" tautomers **a** and **b** and represents an "enol–enol" interconversion via a proton transfer along the intramolecular hydrogen bond of 3-acetyl tetronic acid. In a similar way, structure **c–d TS** connects "internal" tautomers **c** and **d**. Structure
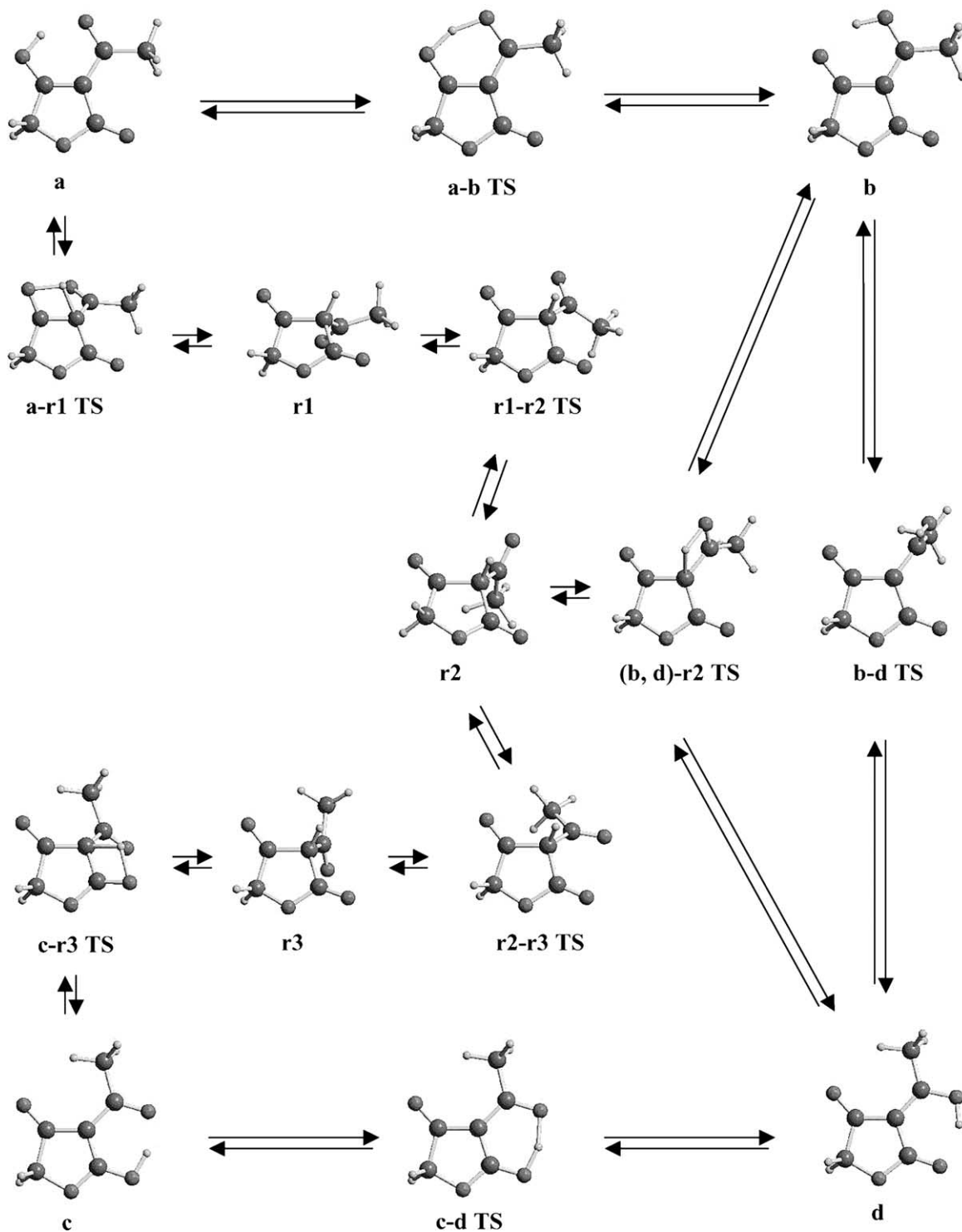
Fig. 3. The mechanism of the tautomerisation reactions of 3-acetyl tetronic acid including the transition state for each step.

b–d TS connects **b** to **d** through a rotation of the acetyl side chain C–C double bond. Structures **a–r1 TS** and **c–r3 TS** connect **a** to **r1** and **c** to **r3**, respectively, in the conventional fashion of the "keto–enol" transformation by which a hydrogen atom "jumps" from the hydroxy group to the vinyl β-carbon. In this respect they are equivalent to the transition state for the tautomerisation reaction between vinyl alcohol and acetaldehyde [31]. Structure (**b**, **d**)–**r2 TS** connects **b** and **d** to **r2** and also represents a keto–enol transition in the conventional sense. Finally, by scanning the C7–C6–C3–C4 dihedral angle (see Fig. 1) structures **r1–r2 TS** and **r2–r3 TS** are obtained which connect **r1** to **r2** and **r2** to **r3**, respectively.

Structures equivalent to each equilibrium and transition state of Fig. 3 were also obtained for 3-acetyl tetramic acid, including the rotamer **r3** that Broughton and Woodward were not able to converge with their AM1 calculations.

The relative energies of the 3-acetyl tetronic acid structures of Fig. 3 and of the equivalent 3-acetyl tetramic acid structures are given in Table 1. The AM1 results of Broughton and Woodward are also shown for comparison. The B3LYP and the MP2 energy differences are in very good agreement for the structures that have the same amount of conjugation with structure **d** which is taken as the

zero of energy. On the other hand, there are disagreements of the order of 10 kJ/mol or more between B3LYP and MP2 for the structures with different amount of conjugation from **d**. One such example is the 3-acetyl tetronic acid structure **r1** (no alternating single and double bonds, hence no conjugation) which is higher in energy than **d** (conjugation due to planar geometry with alternating single and double bonds) by 58.3 kJ/mol according to B3LYP but only 27.8 kJ/mol according to MP2. This discrepancy arises because currently available density functional methods overestimate the stability of conjugated systems, as has been established with calculations on a variety of cases [32,33]. We should therefore consider the MP2 results as the most reliable since the MP2 method is not prone to this weakness.

On the basis of the energy separations we could classify the equilibrium structures into a low energy group of **a**, **b**, **c** and **d** tautomers that would be the form in which the majority of the molecules are present at room temperature and a higher energy group of **r1**, **r2** and **r3** tautomers that would be present only in trace amounts. This distinction applies equally well to the 3-acetyl tetronic acid and to the 3-acetyl tetramic acid as the substitution of the O atom by the isoelectronic N–H unit shifts the energy of each tautomer by a few kJ/mol but

Table 1
Energies (kJ/mol) of 3-acetyl tetronic and 3-acetyl tetramic acid structures (relative to tautomer **d** which is taken as the zero of energy) as calculated with the B3LYP and MP2 methods using the pTZV basis and with the AM1 method [21]

Structure	3-Acetyl tetronic acid			3-Acetyl tetramic acid		
	B3LYP	MP2	AM1	B3LYP	MP2	AM1
a	9.2	3.8	28.1	16.0	10.7	32.7
a–b TS	19.7	17.9	–	25.7	23.0	–
b	2.0	2.6	−0.8	5.5	5.7	3.3
b–d TS	170.0	181.1	–	187.2	196.3	–
d	0.0	0.0	0.0	0.0	0.0	0.0
d–c TS	23.0	21.5	–	18.2	17.7	–
c	21.1	19.6	39.4	16.6	16.4	31.0
a–r1 TS	339.4	319.5	–	337.8	317.7	–
(b, d)–r2 TS	252.1	236.4	–	258.1	242.4	–
c–r3 TS	331.6	311.7	–	314.3	293.2	–
r1	58.3	27.8	21.8	52.5	21.6	15.9
r1–r2 TS	71.2	44.2	–	67.2	39.7	–
r2	66.1	38.6	25.5	61.4	33.2	21.4
r2–r3 TS	77.0	50.8	–	74.8	48.1	–
r3	60.0	31.4	23.4	55.7	26.6	–

retains the division into two groups. The enolic tautomers **a**, **b**, **c** and **d** are stabilised by their intramolecular hydrogen bond. The strength of this hydrogen bond, however, should decrease with increasing tautomer stability, as has been demonstrated by experimental and theoretical studies on molecules with double-minimum low-barrier hydrogen bonds [34]. The transition states **r1–r2 TS** and **r2–r3 TS**, not mentioned in the first paper of Broughton and Woodward, represent barriers of rotation along a single C–C bond and as such they are of much lower energy than **a–r1 TS** and **c–r3 TS** which involve breaking/formation of O–H and C–H bonds.

Our calculations confirm that the 3-acetyl tetronic acid and 3-acetyl tetramic acid interconversions **a** = **b** and **c** = **d** are rapid at room temperature as the energy barriers separating these pairs of tautomers are of the same order of magnitude as $K_B T$. On the other hand, the interconversion between the pairs (**a**, **b**) and (**c**, **d**) will be much slower at room temperature, in accordance with previous experimental observations [20]. We should notice that the interconversion between the "external" tautomers (**a**, **b**) and (**c**, **d**) takes place through a rotation of the acetyl side chain (structure **b–d TS**). The alternative path through transition state structure (**b**, **d**)–**r2 TS** that was originally postulated as an intermediate [20] is higher in energy by about 60 kJ/mol, even though it involves rotation through an essentially single C–C bond.

All three tetronic acid transition state structures **a–r1 TS**, (**b**, **d**)–**r2 TS** and **c–r3 TS** represent a keto–enol transition, however, (**b**, **d**)–**r2 TS** is at least 70 kJ/mol or more lower in energy than the rest due to its rotational freedom along the C3–C6 bond (see Fig. 1). In the other two structures the equivalent bonds participate in the ring so their ability to rotate and obtain a favourable conformation during the transition state is severely limited. Therefore the most favourable path to pure keto forms should be through transition state (**b**, **d**)–**r2 TS** and consequently through enol tautomers **b** and **d**. Similar conclusions can be reached for 3-acetyl tetramic acid.

The effect of finite temperature on the energies of tautomers **a**, **b**, **c** and **d** was examined by calculating their relative Gibbs free energies [35] (using the common approximations of ideal gas, rigid rotor and harmonic oscillator) which are shown in Table 2 along with their predicted mole fractions. The energy separation of the tautomers is substantially different from the zero temperature case and therefore the consideration of thermal effects is necessary in order to reach good agreement with the experimental mole fraction estimates which are also given in Table 2.

The frontier orbitals of the tautomers give descriptive information about their reactivity. In Fig. 4 we show contours of the highest occupied molecular orbital (HOMO) and lowest unoccupied molecular orbital (LUMO) of the **d** and **r2** tautomers of 3-acetyl tetronic and 3-acetyl tetramic acid. The HOMO of **d** has mainly π-bonding character and its magnitude is large above and below C3 (see Fig. 1 for the atom numbering scheme) which indicates that this area of the molecule would have an affinity for reaction with electrophiles. The LUMO orbital **d** defines the regions of the molecule where attack by nucleophiles is favoured. The HOMO of **r2** on the contrary has mainly σ-bonding character and is not available to reactants. The LUMO of **r2** indicates that the carbonyl carbon atoms are available for

Table 2

Gibbs free energy differences and predicted mole fractions ($T = 298.15$ K, $p = 1$ atm) for 3-acetyl tetronic and 3-acetyl tetramic acid tautomers **a**, **b**, **c** and **d**. The values in parentheses are estimates derived by analysis of NMR spectra by the method of Nolte et al. [20]

Tautomer	3-Acetyl tetronic acid		3-Acetyl tetramic acid	
	ΔG (kJ/mol)	Fraction (%)	ΔG (kJ/mol)	Fraction (%)
a	−0.85	48.7 (34)	9.27	2.1 (5)
b	1.82	16.6 (26)	5.27	10.3 (15)
c	14.15	0.1 (0)	10.95	1.0 (0)
d	0.00	34.6 (40)	0.00	86.6 (80)

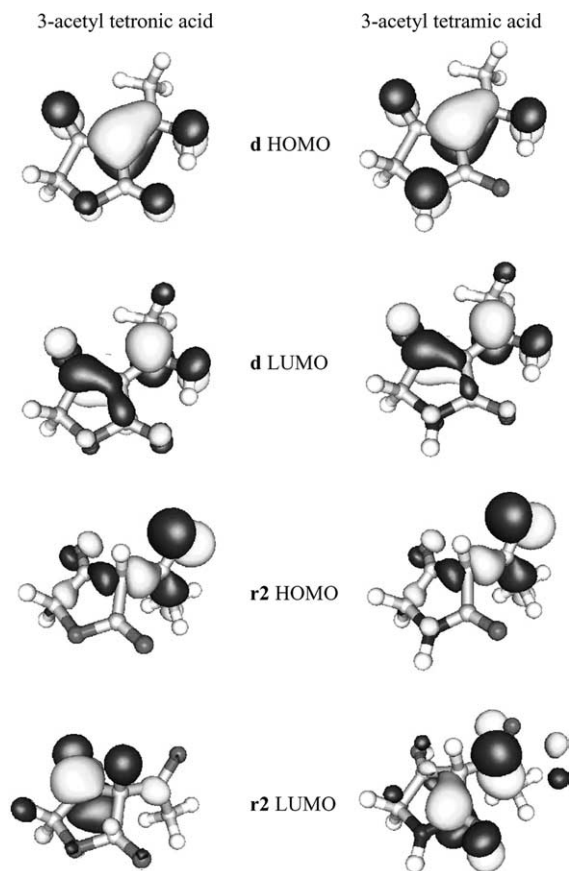3-acetyl tetronic acid   3-acetyl tetramic acid

Fig. 4. Highest occupied molecular orbital (HOMO) and lowest unoccupied molecular orbital (LUMO) of the **d** and **r2** tautomers of 3-acetyl tetronic acid (left) and 3-acetyl tetramic acid (right).

nucleophilic attack albeit not as much as in the case of **d**. In general it is expected that the predominant singly enolised forms of the acids would display larger chemical reactivity than the unenolised keto forms.

A great amount of the experimental information on the equilibrium concentrations of the tautomers is obtained from NMR spectroscopy, therefore the ability to predict NMR spectra provides us with a very effective way of explaining and complementing experimental observations. The ^{1}H and ^{13}C NMR chemical shifts were calculated for the predominant tautomers **a**, **b**, **c** and **d** of 3-acetyl tetronic (Table 3 referring to the atom numbering scheme in Fig. 1) and 3-acetyl tetramic acid (Table 4) and are compared with experimental values. Due to the fast exchange between the pairs of "internal" tautomers that we mentioned above, the experimental values are actually weighted averages for the (**a**, **b**) pair and for the (**c**, **d**) pair and therefore our calculated values are based on this assumption. There is good agreement between the calculated and experimental ^{13}C chemical shifts of 3-acetyl tetronic acid which confirms the experimental assignment of spectra. One point to note here is that in the case of tautomer **d** (for both, 3-acetyl tetronic and 3-acetyl tetramic acids) the experimental assignments of the chemical shifts of C4 and C6 would agree better with the calculated values if their order was switched. There is reasonable agreement between the calculated and the

Table 3
^{1}H and ^{13}C NMR chemical shifts in ppm, relative to TMS as calculated with the GIAO SCF method and the pTZV basis for the (**a**, **b**) and (**c**, **d**) tautomers of 3-acetyl tetronic acid. The numbering scheme for the atoms is shown in Fig. 1. Experimental values are also given for comparison

Atoms	Tautomers **a**, **b**		Tautomers **c**, **d**	
	GIAO SCF	Exp. [36]	GIAO SCF	Exp. [36]
H11, H12	4.18	4.67	4.08	4.56
H13, H14, H15	2.51	2.55	2.60	2.56
H16	15.03	10.51	14.34	10.51
C2	175.9	168.4	188.6	176.6
C3	100.8	100.7	94.6	97.8
C4	211.7	198.1	201.8	192.5
C5	61.0	68.8	68.4	73.7
C6	214.2	194.2	206.8	188.4
C7	24.8	22.0	17.7	19.6

Table 4
^{1}H and ^{13}C NMR chemical shifts in ppm, relative to TMS as calculated with the GIAO SCF method and the pTZV basis for the (**a, b**) and (**c, d**) tautomers of 3-acetyl tetramic acid. The numbering scheme for the atoms is shown in Fig. 1. Experimental values are also given for comparison

Atoms	Tautomers **a, b**		Tautomers **c, d**	
	GIAO SCF	Exp. [37]	GIAO SCF	Exp. [37]
H11, H12	3.45	3.94	3.34	3.81
H13, H14, H15	2.59	2.50	2.54	2.45
H16	14.87	11.59	15.34	11.59
H17	4.17	6.81	4.44	6.88
C2	178.7	170.3	189.1	176.1
C3	101.6	105.2	97.6	101.8
C4	214.9	199.0	201.8	193.1
C5	44.6	48.5	48.1	51.7
C6	207.1	189.4	204.0	185.4
C7	18.7	20.4	17.7	19.5

experimental ^{1}H chemical shifts excluding the enolic proton H16 whose chemical shift is known to be highly dependent on the concentration of solutions. For the 3-acetyl tetramic acid NMR chemical shifts there is also reasonable agreement with the experimental values shown in Table 4.

The tautomers of 3-acetyl tetronic and 3-acetyl tetramic acids are isoelectronic and rather similar from a chemical point of view. They differ in that the 3-acetyl tetronic acid tautomers contain an oxygen atom in position 1 while the 3-acetyl tetramic acid tautomers contain an NH unit in its place. This difference appreciably affects the relative energy ordering of the tautomers of each acid and it has a substantial effect on the relative proportions of the abundant tautomers.

4. Conclusions

We have presented detailed mechanisms of the tautomerisation reactions of 3-acetyl tetronic and 3-acetyl tetramic acids. The equilibrium and transition state structures (that are involved in the mechanisms) were obtained along with their relative energies. Tautomers **a**, **b**, **c** and **d** are the most stable and are the forms in which essentially all of the molecules are present. The relative proportions of the tautomers, however, vary greatly when comparing 3-acetyl tetronic to 3-acetyl tetramic acid and this is clearly the effect of having the oxygen furanone atom in place of the isoelectronic

NH group. We found that the interconversion between "external" tautomers (**a**, **b**) and (**c**, **d**) does indeed take place through the rotation of the acetyl double bond of **b** to yield **d**. We have also determined the three unenolised rotamer equilibrium structures **r1**, **r2** and **r3** of each acid and the transition states that lead to them. Our calculated mole fractions and NMR chemical shifts for **a**, **b**, **c** and **d** tautomers are in good agreement with experiment.

References

[1] D. Pattenden, Fortschr. Chem. Org. Naturst. 35 (1978) 133.
[2] B.J.L. Royles, Chem. Rev. 95 (1995) 1981.
[3] F. Tomita, T. Tamaoki, K. Shirahata, M. Kasai, M. Morimoto, S. Ohkubo, K. Mineura, S. Ishii, J. Antibiot. 33 (1980) 668.
[4] T. Kusumi, A. Ichikawa, H. Kakisawa, M. Tsunakawa, M. Konishi, T. Oki, J. Am. Chem. Soc. 113 (1991) 8947.

[5] T. Hamaguchi, T. Sudo, H. Osada, FEBS Lett. 372 (1995) 54.

[6] S. Aoki, K. Higuchi, Y. Ye, R. Satari, M. Kobayashi, Tetrahedron 56 (2000) 1833.

[7] J.Y. Li, G. Strobel, J. Harper, E. Lobkovsky, J. Clardy, Org. Lett. 2 (2000) 767.

[8] K. Schmidt, U. Riese, Z. Li, M. Hamburger, J. Nat. Prod. 66 (2003) 378.

[9] O. Igglessi-Markopoulou, C.J. Sandris, Heterocycl. Chem. 22 (1985) 1599.

[10] A. Detsi, M. Micha-Screttas, O. Igglessi-Markopoulou, J. Chem. Soc., Perkin Trans. 1 (1998) 2443.

[11] A. Detsi, J. Markopoulos, O. Igglessi-Markopoulou, Chem. Commun. (1996) 1323.

[12] G. Athanasellis, O. Igglessi-Markopoulou, J. Markopoulos, Synletters (2002) 1736.

[13] C.A. Mitsos, A.L. Zografos, O. Igglessi-Markopoulou, J. Org. Chem. 65 (2000) 5852.

[14] C.A. Mitsos, A.L. Zografos, O. Igglessi-Markopoulou, J. Heterocycl. Chem. 39 (2002) 1201.

[15] A. Detsi, V. Bardakos, J. Markopoulos, O. Igglessi-Markopoulou, J. Chem. Soc., Perkin Trans. 1 (1996) 2909.

[16] O. Markopoulou, J. Markopoulos, D. Nichols, J. Inorg. Biochem. 39 (1990) 307.

[17] B.T. Heaton, C. Jacob, J. Markopoulos, O. Markopoulou, J. Nähring, C.-K. Skylaris, A.K. Smith, J. Chem. Soc., Dalton Trans. (1996) 1701.

[18] E. Gavrielatos, C. Mitsos, G. Athanasellis, B.T. Heaton, A. Steiner, J.F. Bickley, O. Igglessi-Markopoulou, J. Markopoulos, J. Chem. Soc., Dalton Trans. (2001) 639.

[19] S. Gelin, P. Pollet, Tetrahedron Lett. 21 (1980) 4491.

[20] M.J. Nolte, P.S. Steyn, P.L. Wessels, J. Chem. Soc., Perkin Trans. 1 (1980) 1057.

[21] H.B. Broughton, P.R. Woodward, J. Comput.-Aided Mol. Des. 4 (1990) 147.

[22] M.J.S. Dewar, E.G. Zoebisch, E.F. Healy, J.J.P. Stewart, J. Am. Chem. Soc. 107 (1985) 3902.

[23] A.D. Becke, J. Chem. Phys. 98 (1993) 5648; P.J. Stevens, F.J. Devlin, C.F. Chabalowski, M.J. Frisch, J. Phys. Chem. 98 (1994) 11623.

[24] J. Baker, P. Pulay, J. Chem. Phys. 117 (2002) 1441.

[25] A. Schäfer, H. Horn, R. Ahlrichs, J. Chem. Phys. 97 (1992) 2571.

[26] A. Schäfer, C. Huber, R. Ahlrichs, J. Chem. Phys. 100 (1994) 5829.

[27] R.J. Harrison, J.A. Nichols, T.P. Straatsma, M. Dupuis, E.J. Bylaska, G.I. Fann, T.L. Windus, E. Apra, W. de Jong, S. Hirata, M.T. Hackler, J. Anchell, D. Bernholdt, P. Borowski, T. Clark, D. Clerc, H. Dachsel, M. Deegan, K. Dyall, D. Elwood, E. Glendening, M. Gutowski, K. Hirao, A. Hess, J. Jaffe, B. Johnson, J. Ju, R. Kendall, R. Kobayashi, R. Kutteh, Z. Lin, R. Littlefield, X. Long, B. Meng, T. Nakajima, J. Nieplocha, S. Niu, M. Rosing, G. Sandrone, M. Stave, H. Taylor, G. Thomas, J. van Lenthe, K. Wolinski, A. Wong, Z. Zhang, NWChem, A Computational Chemistry Package for Parallel Computers, Version 4.1, Pacific Northwest National Laboratory, Richland, Washington 99352-0999, USA, 2002.

[28] R. Ditchfield, Mol. Phys. 27 (1974) 789.

[29] T. Helgaker, H.J. Aa. Jensen, P. Jørgensen, J. Olsen, K. Ruud, H. Ågren, A.A. Auer, K.L. Bak, V. Bakken, O. Christiansen, S. Coriani, P. Dahle, E.K. Dalskov, T. Enevoldsen, B. Fernandez, C. Hättig, K. Hald, A. Halkier, H. Heiberg, H. Hettema, D. Jonsson, S. Kirpekar, R. Kobayashi, H. Koch, K.V. Mikkelsen, P. Norman, M.J. Packer, T.B. Pedersen, T.A. Ruden, A. Sanchez, T. Saue, S.P.A. Sauer, B. Schimmelpfenning, K.O. Sylvester-Hvid, P.R. Taylor, O. Vahtras, DALTON, a molecular electronic structure program, Release 1.2, 2001.

[30] T. Helgaker, M. Jaszunski, K. Ruud, Chem. Rev. 99 (1999) 293.

[31] J. Baker, M. Muir, J. Andzelm, J. Chem. Phys. 102 (1995) 2063.

[32] G.A. Jones, M.N. Paddon-Row, M.S. Sherburn, C.I. Turner, Org. Lett. 4 (2002) 3789.

[33] C.H. Choi, M. Kertesz, A. Karpfen, Chem. Phys. Lett. 276 (1997) 266.

[34] P. Gilli, V. Bertolasi, L. Pretto, A. Lyèka, G. Gilli, J. Am. Chem. Soc. 124 (2002) 13554.

[35] All contributions to the Gibbs Free energies were obtained by frequency calculations at the B3LYP pVDZ level on the B3LYP pVDZ optimised geometries and added to the MP2 pTZV//B3LYP pVDZ energies as the geometry optimisation and frequency calculation at the MP2 pTZV level would result in a prohibitive computational overhead.

[36] C. Mitsos, A. Zografos, O. Igglessi-Markopoulou, J. Heterocycl. Chem. 39 (2002) 1201.

[37] Recorded on a Varian Gemini 2000 300 MHz spectrometer ($CDCl_3$ solution).